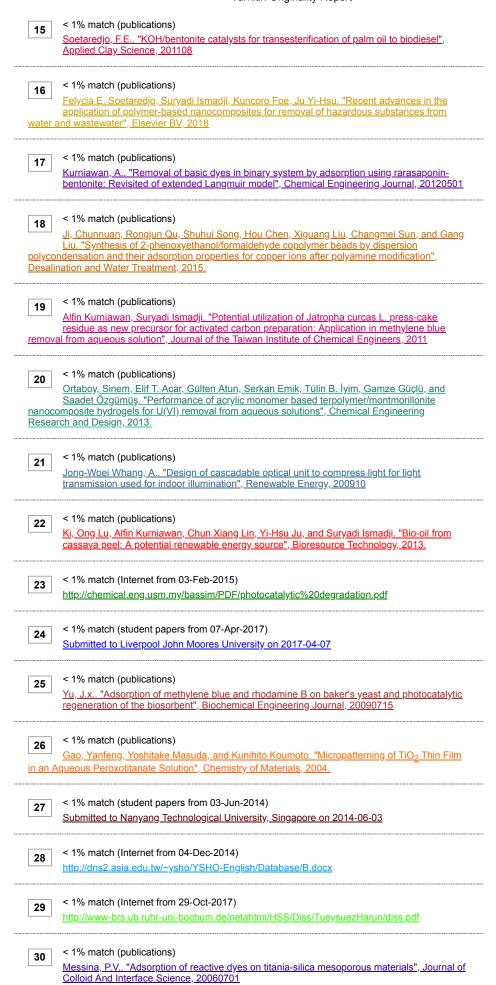
turnitin Originality Report

Heliyon by Suryadi Ismadji From Hippo (Hippo-03)

> Processed on 21-Aug-2018 07:24 WIB ID: 991662365 Word Count: 8231

Similarity by Source Similarity Index 13% 21% 4% Internet Sources: Publications: Student Papers: 21%

sources: 4% match (Internet from 21-Jul-2018) 1 https://orbi.uliege.be/bitstream/2268/226583/1/AE%20v4.pdf 2% match (publications) 2 Mizuho Nishio, Chihiro Nagashima, Saori Hirabayashi, Akinori Ohnishi et al. "Convolutional auto-encoder for image denoising of ultra-low-dose CT", Heliyon, 2017 2% match (publications) Woldegiorgis, Bereket H.. "Egocentric distance perception and performance of direct pointing in stereoscopic displays.(Report)(Author abstract)", Applied Ergonomics 1% match (Internet from 22-May-2011) 4 http://asia.edu.tw/~vsho/Truth/PDF/922313B242007.pdf 1% match (Internet from 30-Aug-2017) 5 https://repositorio-aberto.up.pt/bitstream/10216/11197/2/Texto%20integral.pdf 1% match (Internet from 10-Mar-2016) 6 http://www.mdpi.com/1996-1944/7/1/333/pdf 1% match (publications) 7 Yang, Shubin, Dadong Shao, Xiangke Wang, Guangshun Hou, Masaaki Nagatsu, Xiaoli Tan, Xuemei Ren, and Jitao Yu. "Design of Chitosan-Grafted Carbon Nanotubes: Evaluation of How the -OH Functional Group Affects Cs+ Adsorption", Marine Drugs, 2015. 1% match (publications) 8 Belessi, V.. "Removal of Reactive Red 195 from aqueous solutions by adsorption on the surface of TiO"2 nanoparticles", Journal of Hazardous Materials, 20091030 1% match (publications) Mittal, Hemant, and Suprakas Sinha Ray. "A study on the adsorption of methylene blue onto gum ghatti/TiO2 nanoparticles-based hydrogel nanocomposite", International Journal of Biological Macromolecules, 2016. < 1% match (student papers from 10-Apr-2018) 10 Submitted to Higher Education Commission Pakistan on 2018-04-10 < 1% match (publications) 11 Southichak, B.. "Phragmites australis: A novel biosorbent for the removal of heavy metals from aqueous solution", Water Research, 200607 < 1% match (publications) 12 Huang, Kai, Jiangting Wang, Shuqiang Jiao, and Hongmin Zhu. "Fast removal of dyes from wastewater by combinatorial treatment by biosorption and visible light photodegradation", 2013 International Conference on Materials for Renewable Energy and Environment, 2013. < 1% match (Internet from 01-May-2015) 13 http://tsukuba.repo.nii.ac.jp/index.php? action=pages_view_main&active_action=repository_action_common_download&item_id=24454&item_no=1&attribute_id=17&file_no=1& < 1% match (Internet from 17-Nov-2010) 14 http://lib.jinr.ru/sw43.html



https://www.turnitin.com/newreport_printview.asp?eq=1&eb=1&esm=15&oid=991662365&sid=0&n=0&m=0&svr=21&r=15.899766255951686&lang=e... 2/18

< 1% match (publications) 31

Ismadji, Suryadi, Felycia Edi Soetaredjo, and Aning Ayucitra. "The Equilibrium Studies in the Adsorption of Hazardous Substances Using Clay Minerals", SpringerBriefs in Molecular Science, 2015.

< 1% match (publications) 32

Bouatay, Feriel, Sonia Dridi-Dhaouadi, Neila Drira, and Mohamed Farouk Mhenni. Application of modified clays as an adsorbent for the removal of Basic Red 46 and

< 1% match (student papers from 08-Mar-2018) 33

Submitted to University of Technology, Sydney on 2018-03-08

< 1% match (publications) 34

Laleh Adlnasab, Meisam Shabanian, Maryam Ezoddin, Akram Maghsodi. "Amine rich functionalized mesoporous silica for the effective removal of alizarin yellow and phenol red dyes from waste waters based on response surface methodology", Materials Science and Engineering: B, 2017

< 1% match (publications) 35

Xue Song Wang, Hai Jie Lu, Lei Zhu, Fei Liu, Jun Jun Ren. "Adsorption of Lead(II) lons onto Magnetite Nanoparticles", Adsorption Science & Technology, 2010

< 1% match (publications) 36

Rahardjo, A.K.. "Modified Ponorogo bentonite for the removal of ampicillin from wastewater", Journal of Hazardous Materials, 20110615

< 1% match (student papers from 21-Oct-2005) 37 Submitted to University of Sheffield on 2005-10-21

< 1% match (Internet from 03-Jun-2018) https://www.tandfonline.com/doi/full/10.1080/19443994.2013.811114

paper text:

38

Received: 16 July 2017 Revised: 10 October 2017 Accepted: 7 December 2017 Cite as: Livy Laysandra, Meri Winda Masnona Kartika Sari, Felycia Edi Soetaredjo, Kuncoro Foe, Jindrayani Nyoo Putro, Alfin Kurniawan, Yi-Hsu Ju, Suryadi Ismadji. Adsorption and photocatalytic performance of bentonite- titanium dioxide composites for methylene blue and rhodamine B decoloration. Heliyon 3 (2017) e00488. doi: 10.1016/j.heliyon.2017. e00488 Adsorption and photocatalytic performance of bentonite-titanium dioxide composites for methylene blue and rhodamine B decoloration Livy Laysandra a, Meri Winda Masnona Kartika Sari a, Felycia Edi Soetaredjo a,*, Kuncoro Foe b, Jindrayani Nyoo Putro c, Alfin Kurniawan c,

22Yi-Hsu Ju c, Suryadi Ismadji a,* a Department of Chemical Engineering, Widya Mandala Surabaya Catholic University, Kalijudan 37, Surabaya 60114, Indonesia b Faculty of

Pharmacy, Widya Mandala Surabaya Catholic University, Pakuwon City, Kalisari 1, Surabaya 60112, Indonesia c

21Department of Chemical Engineering, National Taiwan University of Science and Technology, No. 43, Sec 4, Keelung Rd, Da'an District, Taipei City 106, Taiwan * Corresponding author.

E-mail addresses: felyciae@yahoo.com (F.E. Soetaredjo), suryadiismadji@yahoo.com (S. Ismadji). Abstract Bentonite - TiO2 composites were prepared by impregnation of TiO2 and bentonite, followed by microwave irradiation processes. The composites were characterized using FTIR, SEM, XRD, and nitrogen sorption methods. Anatase phase of TiO2 in all composites are observed through XRD diffraction peaks and surface morphology of the composites. The adsorption and photocatalytic capabilities of the composites were tested in liquid phase adsorption of methylene blue and Rhodamine B. The adsorption and photocatalytic degradation experi- ments were conducted in the presence or absence of UV light irradiation. Langmuir and Freundlich models were employed to correlate the experimental adsorption data, and it was found that

Langmuir gave better performance in correlating the experimental data. Modification of Langmuir equation to accommodate

3http://dx.doi.org/10.1016/j. heliyon .2017.

e00488 2405-8440/©

22017 The Authors. Published by Elsevier Ltd.

This is an open access article

1under the CC BY-NC-ND license (http://creativecommons.org/licenses/bync-nd/4.0/).

photocatalytic degradation process was conducted, and the model could represent the experimental results very well. Keywords: Environmental science, Materials science, Chemical engineering 1. Introduction Dyes usually used by various kinds of industries to color their products. Several industries that intensively use dyes to color their products are textiles, foods, pharmaceuticals, cosmetics, paints, pigments, ceramics, etc. During the industrial processing, some of the excess dyes will end up as waste and will be discharged as industrial effluent [1]. Industrial effluents containing dyes are dangerous to the aquatic environment as well as to human being. Therefore, a proper treatment should be conducted before these kinds of effluents can be discharged to the water environment. The principal purposes of the treatment are to remove inorganic or organic contaminants, and other pathogens microorganisms from water, so human for their daily activities can safely use the water. Different kinds of dyes, mostly are synthetic ones, are commercially available in the markets. Synthetic dyes are classified into several categories: basic or cationic dyes, the direct dyes, the

16acid dyes, premetallized dyes, sulfur dyes, azoic dyes, vat dyes, collective dyes, and dyes

for fabricated fibers. Basic dyes are water-soluble cationic dyes applied to substrate with anionic character where electrostatic attractions are formed. Some examples of basic dyes are Methylene Blue, Rhodamine B Crystal Violet, Congo Red, Methyl Orange, etc. [2]. Some of these synthetic dyes have been known to have

9potential hazards to human health, and their effect is mainly carcinogenic, mutagenic and teratogenic

[3]. Methylene blue is known as methylthioninium chloride is a basic cationic dye

24with the molecular formula C16H18N3SCI. At room temperature, methylene blue is solid, odorless, dark green powder and gives blue solution if dissolved in water. This dye is

usually used in biological and chemical processes [4]. Rhodamine B is a basic cationic dye with the molecular formula C28H31CIN2O3 has a moderate wash and light fastness properties of wool. It is also useful as an analytical reagent for the detection and determination of metals [5, 6, 7]. Methylene blue can cause some health problems such as

6eye burns, which may be responsible for permanent injury to the eyes of human and animals. On an inhalation, it can give short periods of rapid or difficult breathing, while ingestion through the mouth gives a burning sensation and may cause nausea, vomiting, profuse sweating, mental confusion, and methemoglobinemia [8]. The long-term exposure of

Rhodamine B to human may cause in transient mucous membrane and skin irritation. Rhodamine B potentially induces mutagenic activity and pose an adverse effect on aquatic life via obstructing light penetration and oxygen transfer [9]. Many dyes and other organic contaminants are tough to degrade in nature and require more advanced techniques for their removal [1]. The decolorization of dye

8has received much attention. Thus various chemical, physical and biological treatment methods have been developed for the removal of dyes from aqueous solutions. These treatments include precipitation, coagulationflocculation, reverse osmosis, oxidation with ozone, chlorine or hydrogen peroxide, use of anion exchange membranes and bacterial cells [10]. Adsorption

9is one of the most promising and widely used techniques for the removal synthetic dyes from wastewater [3].

Adsorption has proven to be a promising and cost-effective method. The price of

34adsorbent is an important parameter that significantly influences the total cost of

an adsorption process system. Therefore the search of alternative adsorbents with high adsorption capacities was still the focus of current studies [11]. Many kinds of non-conventional adsorbent materials have been tested for their adsorption ability to remove dyes. As alternative adsorbents, non-conventional materials must possess similar adsorption capability to those commercial adsorbents, eco-friendly production, and also abundantly available [12]. The most promising and the materials as the candidate for alternative adsorbents are clay minerals. Bentonite is a clay material that can be found in many places around the world, including in Indonesian. Bentonite is a smectite mineral composed of aluminum silicate framework, and it has a layer structure with negative charge evenly across its surface and possesses good cation exchange. In the last few years, the study of decolorization of dyes using photocatalytic process has been investigated [13]. Among different kinds of photocatalysts, TiO2 is the most widely used for wastewater treatment because of its high oxidizing properties, super hydrophilicity and chemical stability [14]. However, this process requires UV-light radiation to promote the

37electron from the valence band to the conduction band and leave the hole (h +) in the valence band.

If the hole meets the water molecule in the presence of oxygen, it will produce hydroxyl radical (OH●), and this hydroxyl radical will break down the organic molecule into the simple compound [13]. The main drawback of using titanium as a photocatalyst is its susceptibility to aggregation, reducing the surface area and efficiency [1]. To avoid this problem, a suitable material as the support to immobilize titanium particles should be developed, and clay materials are good candidates for this purpose [1]. In this study, bentonite was employed as the support to immobilize TiO2 particles. The bentonite - TiO2 composite was subsequently used to adsorb and degrade

25Methylene Blue and Rhodamine B. The adsorption, and photodegradation performances of the

adsorbents were observed at various temperatures. Since

25the removal of Methylene Blue and Rhodamine B

involves both of adsorption and photodegradation, a modification of Langmuir equation was also conducted to represent the photo-degradation term.

152. Materials and methods 2.1. Materials Ca -Bentonite used in this study was obtained from Pacitan, East Java, Indonesia.

Titanium dioxide (anatase phase) was purchased from Degussa.

28Methylene Blue (MB) and Rhodamine B (RhB) were purchased from

Merck, Germany. 2.2. Preparations of bentonite-titanium dioxide composite Before use as the adsorbent, the bentonite was purified using H2O2 solution. The purification of bentonite was conducted to remove organic impurities. The purification was carried out in a sonicator for 6 hours at room temperature. After the purification process had completed, bentonite was separated from the solution and

17repeatedly washed with reverse osmosis water and dried in a forced circulation oven (Memmert) at 105 °C for

24 h. The purified bentonite was pulverized in a hammer mill and sieved using vibration screener (Retsch AS-200)

36to obtain a particle size of 100/120 mesh.

Bentonite titanium dioxide nanocomposites (BTC) were synthesized at a different weight ratio of TiO2 (5, 10, 20%) using impregnation method [15]. The impregnation procedure is as follows: a known amount of titanium dioxide was dispersed in water; subsequently, a known amount of bentonite was added to the mixture and heated at 100 °C for 1 hour under continuous stirring. The BTC mixture was then irradiated using a microwave oven at 700W for 10 minutes. After the irradiation process had completed, the BTC was separated from the liquid

13and dried at 105 °C for 24 h.

The radiation process using microwave could improve the adsorption capacity of adsorbent [16].

362.3. Characterizations of materials The characterizations of bentonite and nanocomposites were

conducted using several methods such surface charge, FTIR (Fourier Transform Infra-Red Spectrophotometry), SEM (Scanning Electron Microscopy), and XRD (X-Ray Diffraction). In this study, the surface charge of bentonite and nanocomposites was measured by a zeta meter (Zeta Potential Analyzer, Brookhaven 90Plus). The pHpzc (the pH where the adsorbent has no charge) or isoelectric points of bentonite and nanocomposites were 3.9 (bentonite (B)), 5.2 (B + 5% TiO2), 6.1 (B + 10% TiO2), and 7.6 (B + 20% TiO2). The FTIR analysis of bentonite and nanocomposites were conducted on a Shimadzu FTIR 8400S spectrometer using KBr method. The FTIR spectra of the samples were acquired at a wavenumber of 4000 to 500 cm-1. The FTIR data were collected in transmission mode. The adjustment of the baseline, normalization, and smoothing of the FTIR spectra were conducted using IRsolution software package (version 1.21). This software is available in the FTIR instrument. The surface morphologies of bentonite and titanium nanocomposites were determined by scanning electron microscopy method. The surface analysis was carried out on a JEOL JSM-6500F field emission SEM at 20 kV. Before SEM analysis, the samples were coated with a thin layer of platinum (3 nm). The coating process was conducted for 90 s in argon atmosphere using a fine auto coater (JFC- 1600, JEOL, Ltd., Japan).

20X-ray diffraction patterns of the samples were obtained

at 40 kV and 30 mA using XRD, Philips X'pert X-ray Diffractometer. Monochromatic high-intensity Cu Kα1 (λ = 0.15405 nm) was employed as the source of radiation. The pore structures of the samples were characterized by nitrogen sorption analysis. The nitrogen sorption measurements were conducted at the boiling point of nitrogen gas (-176 °C) using Micromeritics ASAP 2010 sorption analyzer. The adsorption and desorption of the nitrogen were performed

17at relative pressure (p/ p°) range of 0. 005 to 0.995. The degassing of the samples were

conducted at 200 °C under high vacuum condition. 2.4. Adsorption and photocatalytic degradation experiment Adsorption and photocatalytic processes were carried out isothermally in a water bath shaker that has been modified by adding a UV lamp as the light source. The adsorption and photodegradation processes were conducted with an initial concentration of 200 ppm for both MB and RhB. For the isotherm process, the various mass of Ca-bentonite or BTC (0.1 - 0.9 g) were

19added to a series of iodine flasks, each flask containing 100 mL of

MB or RhB solution. The adsorption and photodegradation experiments were performed at three different temperatures (30 °C, 50 °C, and 70 °C) and pH 8. During the experiments, the iodine flasks containing the mixture were shaken in a thermal controlled shaking water bath (Memmert WB-14) with constant speed at 100 rpm for 2 h at desired temperature with/without UV irradiation at 360 nm (To measure the adsorption performance of the composites, the adsorption experiments was conducted in the dark without any light disturbing.). After the adsorption and photodegradation process had completed, samples were centrifuged (Heraeus Labofuge 200) at 3500

34rpm for 2 min to separate the solution from the adsorbent [11]. The

initial and equilibrium concentrations of MB or RhB were determined by UV-Visible spectrophotometer (UV mini 1240 Shimadzu) at the maximum wavelength (664.1 nm for MB and 554.0 nm for RhB). The amount of MB or RhB adsorbed by the adsorbent at equilibrium condition was determined by equation (1) as follow: qe ¼ ðC0 ? CeÞ m ×V (1) Where

32qe is the amount of MB or RhB adsorbed at equilibrium (mmol/g), C0 and

32Ce (mmol/L) represent the concentration of

MB or RhB in the liquid phase at initial and equilibrium condition, respectively. The volume of MB or RhB solution is represented by symbol V

13(L) and m is the mass of adsorbent (g). 3. Results and discussion 3.1.

FTIR analysis In this study, FTIR spectroscopy was used to analyze the functional groups of the adsorbents. Fig. 1. Shows the FTIR spectra of TiO2, bentonite, B + 5%TiO2, B + 10% TiO2, and B + 20% TiO2. Broadband around 500 to 700 cm-1 possibly

26due to the vibration of Ti-O bonds in the titanium dioxide lattice [17]. The

26vibration of hydroxyl groups is observed at

broad peaks around 3100 to 3600 cm-1 (Fig. 1a). Typical infrared absorption bands of montmorillonite are observed on the bentonite (Fig. 1e). Those bands are

15AI(Mg) - O - H stretching (3620 cm -1), intermolecular hydrogen-bonded H - O -H stretching (3343 cm -1), Si -O-

Si stretching vibration at 1113 cm−1, Al-OH (911 cm−1), (Al, Mg)–O (866 cm−1), and Si–O bending vibration (445 cm-1) [18]. Similar infrared absorption bands of montmorillonite and TiO2 are observed for all of the bentonite - TiO2 composites as seen in Fig. 1. Skeletal vibrations of clay particles and TiO2 for all composites are in the wavenumbers between 1200-450 cm-1 [17]. 3.2. Surface morphology analysis The surface morphology of bentonite and composites (B + 5%TiO2, B + 10%TiO2, and B + 20%TiO2) was examined by SEM, and the results are depicted in Fig. 2. From this Figure, it can be seen that bentonite possesses different surface morphology with bentonite - TiO2 composites. The surface morphology of bentonite appears as a flake-like structure with a smooth surface in some part of the particles, while the bentonite - TiO2 composite, some TiO2 particles have been incorporated into the surface of bentonite (smaller TiO2 grains on the outer face of bentonite). The EDS spectra reveal that the composite contains a

significant amount of titanium as indicated in Fig. 2. 3.3. X-ray diffraction Fig. 3 shows the XRD patterns of bentonite and bentonite - TiO2 nanocomposites. Based on the XRD pattern of bentonite, the specific diffraction peak for ([]GIF\$DT)1_.giF (a) 700 - 500 cm-1 (b) (c) 1200 - 450 cm-1 (d) (e) 3624 cm-1 866 cm-1 3620 cm-1 3343 cm-1 911 cm-1 1113 cm-1 -1 445 cm 4000 3000 2000 1000 Fig. 1. FTIR spectra of (a) TiO2, (b) B + 20% TiO2, (c) B + 10% TiO2, (d) B + 5% TiO2, and (e) Ca- bentonite. montmorillonite appears at $2\theta = 5.69^{\circ}$, and this 2θ corresponds to the basal spacing d001 = 15.53 Å. Other characteristic diffraction peaks of montmorillonite were observed at 20 = 19.82°, 27.70°, 34.79°, and 59.64°. The presence of quartz on the bentonite was also observed, and the diffraction peaks of quartz were found at $2\theta = 26.59^{\circ}$ and 50.01°. The specific diffraction peak of montmorillonite in composites was observed at 20 around 5.40° (B+ 5%TiO2), 5,29° (B + 10%TiO2), and 5.19° (B + 20%TiO2). Incorporation of TiO2 into bentonite structure slightly increases the interlayer spacing from 15.53 Å to 16.35 Å (B + 5%TiO2), 16.71 Å (B + 10%TiO2), and 17 Å. The increase of interlayer spacing with the increase of TiO2 ratio possibly due to Fig. 2. SEM images and EDS spectra of (a) bentonite, (b) B + 5% TiO2, (c) B + 10% TiO2, and (d) B + 20% TiO2. the exchanged of Na+ or Ca2+ with TiO2. More TiO2 particles were available with the increase of TiO2 ratio, and more particles penetrated into the bentonite interlayers (due to the ion-exchanged process) increasing interlayer spacing. Anatase phase of TiO2 in all composites are observed through diffraction peaks around 2θ = 25.50° (101), 37.69° (112), 48.15° (200), and 54.99°. This evidence TiO2 anatase Montmorillonite Quartz (101) Bentonite B+5%TiO2 B+10%TiO2 B+20%TiO2 (001) (112) (200) (001) (112) (101) (200) Intensity (001) (101) (112) (200) (001) 10 40 20 30 50 60 70 20,0 Fig. 3. X-ray diffraction of bentonite and composites. indicates that there is no change in the phase of TiO2 during the microwave irradiation process. Anatase phase of TiO2 has much higher photocatalytic activity than other phases of TiO2. 3.4. Nitrogen sorption measurements The nitrogen sorption isotherms for bentonite and bentonite - TiO2 composites are given in Fig. 4. The adsorption isotherm of bentonite (Fig. 4a) indicates that this material possesses some amount of micropore in its structure. Rapid intake of nitrogen gas by the solid at very low relative pressure (p/p°) is the characteristic of the solid that has some microporous structure (type I adsorption isotherm). With the increase of relative pressure, the isotherm becomes type II, and wide hysteresis loop is observed as seen in Fig. 4a. This kind of hysteresis loop can be considered as H2 type hysteresis. This hysteresis indicates that the purification of natural bentonite with concentrated hydrogen peroxide solution created some complex network of interconnected pores or interlayers with bottleneck and contractions [19], and such structure delayed the desorption of nitrogen gas. The BET surface area and pore volume of the bentonite are 68.4 m2/g and 0.126 cm3/g, respectively. The nitrogen sorption isotherms of the composites are given in Fig. 4b, c, and d. The sorption isotherms of composites B + 5% TiO2 and B + 10% TiO2 are similar to the bentonite, combination between type I and II. Type II isotherms indicate that B + 5% TiO2 and B + 10% TiO2 contain both mesoporous and macroporous structures. The BET surface area and pore volume of composite B + 5% TiO2 are 111.7 m2/g and 0.191 cm3/g, respectively, while for B + 10% TiO2 are 141.8 m2/g and 0.218 cm3/g. With the addition of TiO2, some ion exchange process between Na+ and Ca2+ with TiO2 occurred, and some interlayer which initially inaccessible by nitrogen gas now become available due to the penetration of titanium molecules, so it enhances the ([]GIF\$DT)4_.giF 140 0.030 (a) 0.025 120 0.020 0.015 V (cm3/g, STP) 100 dV/dP (cm3/g,nm) 0.010 0.005 80 0.000 1 2 3 4 5 6 7 8 9 60 Pore size, nm V(cm3/g, STP) 40 20 0 0.0 0.2 0.4 0.6 0.8 1.0 p/po 0.07 0.06 (c) 200 V (cm3/g, STP) dV/dP (cm3/g.nm) 0.05 0.04 0.03 0.02 150 0.01 0.00 1 2 3 4 5 6 7 8 9 Pore size, nm 100 V (cm3/g, STP) 50 0.0 0.2 0.4 0.6 0.8 1.0 p/po 200 0.030 150 dV/dP (cm3/g.nm) 0.025 (b) 0.020 0.015 0.010 0.005 0.000 100 1 2 3 4 5 6 7 8 9 Pore size.

27nm 50 0 0.0 0.2 0.4 0.6 0.8 1.0 p/po 300

(d) 0.10 dV/dP (cm3/g.nm) 0.08 250 0.06 0.04 200 0.02 0.00 1 2 3 8 9 4 5 6 7 150

29Pore size, nm 100 50 0 0.0 0.2 0.4 0.6 0.8 1.0 p/

po Fig. 4. Nitrogen sorption isotherms and pore size distribution for (a) bentonite, (b) B + 5% TiO2, (c) B + 10% TiO2, and (d) B + 20% TiO2. adsorption of nitrogen. With the increase of the ratio of TiO2 to 20%, the type of sorption isotherms of the composites change from type I/II to type IV with H3-H4 hysteresis loop as depicted in Fig. 4d. It indicates that B + 20% TiO2 contain non-rigid aggregates of plate-like particles with a contribution of micropores and mesopores [20]. The BET surface area of B + 20% TiO2 composite is 208.6

28m2/g and total pore volume 0. 243 cm3/g. The

pore size distribution (PSD) of bentonite and composites were obtained by

19density functional theory (DFT) with medium regularization; the results

are also given in Fig. 4 (as insert graphics). The PSDs reveal that all of the solids mainly have mesoporous structures. 3.5. Adsorption and photocatalytic performance Analysis of the adsorption isotherm is very crucial for the design of adsorption system. The adsorption isotherm describes how the adsorbate molecules interact with the adsorbent surface at equilibrium condition [21]. Currently, many adsorption isotherm equations are available

31to represent the experimental adsorption data of different systems, and the

19most widely used equations to represent the liquid phase adsorption experimental data

are Langmuir and Freundlich equations. In this study, we also employed Langmuir and Freundlich isotherms to represent the adsorption data of MB and RhB onto bentonite and composites (the adsorption experiments were carried out in the dark place without UV irradiation). The mathematical expressions of Langmuir and Freundlich adsorption models are given in Eqs. (2) and (3): qe ¼ qmax1 þ KLCe KLCe (2) Where qe and Ce are the amount of dyes adsorbed by the adsorbent at equilibrium condition and equilibrium concentration, respectively. The Langmuir parameters qmax and KL represent the maximum adsorption capacity and adsorption affinity. qe 1/4 KFCe1=n (3)

38Where KF and n are Freundlich constants that represent the adsorption capacity of the adsorbent and heterogeneity of the system, respectively. The adsorption

isotherms of MB and RhB onto bentonite and composites are given in Figs. 5 and 6. In this figure, the experimental adsorption data are represented by the symbols, while the theoretical isotherms are given by solid (Eq. (2)) and dash (Eq. (3)) lines. The parameters of Langmuir and Freundlich equation

16obtained from the fitting of the experimental data with the

isotherm models are summarized in Table 1 (MB) and Table 2 (RhB). From Figs. 5 and 6, it is evident that the Langmuir equation can represent the experimental data better than Freundlich equation. Langmuir equation also has better values of R2 compared to Freundlich equation (Tables 1 and 2). 0.18

```
4qe, mmol/g 0. 16 0. 14 0. 12 0. 10 0. 08 0. 06 0. 04 0. 02 0. 00 (a)
```

T = 30oC T = 50oC T = 70oC Langmuir isotherm 0.16 0.0 0.1 0.2 0.3 Ce, mmol/L 0.4 0.5

```
4qe, mmol/g 0.14 0.12 0. 10 0.08 0.06 0.04 0.02 0. 00 (b)
```

0.16 0.0 0.1 0.2 0.3 Ce, mmol/L 0.4 0.5 qe,

```
5mmol/g 0.14 0.12 0.10 0.08 0.06 0.04 0.02 0.00 (c)
```

0.16 0.0 0.1 0.2 0.3 Ce, mmol/L 0.4 0.5

```
4qe, mmol/g 0.14 0.12 0. 10 0.08 0.06 0.04 0.02 0. 00 (d) 0.
```

0 0

```
11.1 0.2 0.3 Ce, mmol/L
```

0.4 0.5 0.20

```
4qe, mmol/g 0. 18 0. 16 0. 14 0. 12 0. 10 0. 08 0. 06 0. 04 0. 02 0.
```

```
00 T = 30oC T = 50oC T = 70oC Freundlich isotherm 0.0 0.18 0.1 0.2 0.3 Ce, mmol/L 0.4 0.5
         30qe, mmol/g 0. 16 0. 14 0. 12 0. 10 0. 08 0. 06 0. 04 0. 02 0. 00 0. 0 0. 16 0. 1 0. 2
         0.
3 Ce, mmol/L 0.4 0.5 qe, mmol
          10/g 0. 14 0. 12 0.10 0. 08 0. 06 0. 04 0. 02 0. 00 0. 0 0. 16 0. 1 0. 2 0. 3 Ce, mmol/L
4 0.5 qe, mmol
          10/g 0. 14 0. 12 0.10 0. 08 0. 06 0. 04 0. 02 0. 00 0. 0 0. 1 0. 2 0. 3 Ce, mmol/L 0.
4 0.5 ([]GIF$DT)6_.giF T = 30oC 0.14 T = 50oC T = 70oC 0.12 Langmuir isotherm
         35(a) (b) 0.12 0.10 0. 14 0. 14 qe, mmol/g 0.08 0.06 0.04
0.02 0.00
          12qe, mmol/g 0.12 0.10 0.08 0.06 0.04 0.02 0.00
0.0 0.1 TT == 3500ooCC T = 70oC Freundlich equation 0.2 0.3 Ce, mmol/L
          11qe, mmol/g 0.08 0.06 0.04 0.02 0.
00
         12qe, mmol/g 0.12 0.10 0.08 0.06 0.04 0.02 0.00
0.0 0.1 0.2
          7Ce, mmol/L 0. 3 0. 0 0. 1 0. 2 0. 3 0. 0 0. 1 0. 2 0.
3 Ce, mmol/L Ce, mmol/L 0.10 0.12 0.12 (c) (d) 0.10 0.10 qe, mmol/g 0.08 0.08 0.12 0.06 0.04 0.10 qe,
mmol/g 0.08 0.06 0.04 qe,
         5mmol/g 0. 06 0. 04 qe, mmol/g 0.12 0.10 0.08 0. 06 0. 04 0. 02 0. 00 0. 02 0. 00 0.
          7Ce, mmol/L 0. 1 0. 2 0.2
         7Ce, mmol/L 0. 3 0. 3 0. 02 0. 00 0. 0 0. 1 0. 02 0. 00 0.
0 Ce, mmol/L 0.1 0.2 0.2 Ce, mmol/L 0.3 0.3 Fig. 6. Experimental and theoretical adsorption isotherms of
```

RhB onto (a) bentonite, (b) B + 5% TiO2, (c) B + 10% TiO2, and (d) B + 20% TiO2. Comparing the adsorption capacity of the solids, without the presence of UV light the ratio of TiO2 on composite did not give any contribution to the adsorption capacity as seen in Tables 1 and 2, the value of qmax for all adsorbents are essentially constant. From Figs. 5 and 6, it can be seen that temperature gives a positive contribution to

the amount of dyes adsorbed by the adsorbents. The amount uptake slightly increases with the increase of temperature. The increase of the adsorption capacity with temperature indicates that the chemisorption controls the adsorption of MB and RhB onto bentonite and composites. Since the Langmuir could represent the experimental adsorption data better than Freundlich model, the Langmuir equation was modified to include the photocatalytic degradation term. With the presence of UV light during the adsorption process, the decrease of the amount of dyes during the process is due to the adsorption and Fig. 5. Experimental and theoretical adsorption isotherms of MB onto (a) bentonite, (b) B + 5% TiO2, (c) B + 10% TiO2, and (d) B + 20% TiO2. Table 1. Langmuir and Freundlich parameters for the adsorption of MB onto bentonite and composites without UV irradiation. Adsorbent

18T(°C) Langmuir Parameters Freundlich Parameters qm (mmol/g) KL (L/mmol) R2 Kf (mmol/g

(mmol/L)-n) n R2 Bentonite B+ 5% TiO2 B+ 10% TiO2 B+ 20% TiO2 30 0.1434 82.06 0.993 50 0.1576 86.09 0.998 70 0.1615 156.09 0.992 30 0.1450 59.94 0.997 50 0.1482 54.96 0.999 70 0.1476 77.12 0.994 30 0 1486 32 31 0 998 50 0 1484 35 34 0 995 70 0 1497 36 47 0 996 30 0 1508 23 02 0 997 50 0 1500 27.89 0.996 70 0.1515 33.14 0.997 0.1741 5.76 0.984 0.1911 5.86 0.977 0.1992 6.36 0.969 0.1850 4.26 $0.942\ 0.1834\ 4.69\ 0.939\ 0.1771\ 5.75\ 0.978\ 0.\ 1813\ 3.93\ 0.958\ 0.1839\ 4.06\ 0.965\ 0.1805\ 4.41\ 0.951\ 0.1768$ 3.95 0.980 0.1810 3.95 0.968 0.1782 4.54 0.982

13Table 2. Langmuir and Freundlich parameters for the adsorption of

RhB onto bentonite and composites without UV irradiation. Adsorbent

18T (°C) Langmuir Parameters Freundlich Parameters qm (mmol/g) KL (L/mmol) R2 Kf (mmol/g

(mmol/L)-n) n R2 Bentonite 30 50 70 0.1078 0.1127 0.1184 272.97 231.65 297.29 0.996 0.996 0.998 0.1350 0.1325 0.1384 7.25 9.03 10.08 0.962 0.975 0.987 B+ 5% TiO2 30 50 70 0.1044 0.1047 0.1102 127.41 174.46 180.14 0.993 0.998 0.999 0.1329 0.1335 0.1335 5.49 6.45 7.81 0.937 0.962 0.978 B+ 10% TiO2 30 50 70 0.0963 0.0978 0.0997 120.97 130.29 149.38 0.992 0.993 0.998 0.1218 0.1234 0.1214 6.07 6.28 7.41 0.968 0.970 0.975 Be+ 20% TiO2 30 50 70 0.0957 0.0971 0.0983 80.81 91.11 123.05 0.999 0.998 0.997 0.1211 0.1239 0.1241 5.19 5.31 5.62 0.983 0.980 0.987 photocatalytic degradation processes. Before the photocatalytic degradation process occurs, the first process is the adsorption of dye molecules on the surface of the composite. When the dye molecules adsorbed on the surface near the TiO2 particles, with the presence of UV light, the photocatalytic degradation process occurs. The degradation process is initiated by the excitation of

23an electron from the valence band of the TiO2 catalyst to the conduction band, thus generating a hole (h+) in the valence band

and make ●OH radical when contacted with water. Subsequently, the ●OH radical attacks dye molecule and degradation process occur. After the degradation of dye molecule has finished, some of the degradation product will be released to water, and some possibly remain adsorbed on the surface of the adsorbent. This process continues until the product of degradation covers the TiO2 particle and become deactivated. However, if dye molecules are adsorbed on the surface far from the location of TiO2 particle, the photocatalytic degradation process will not occur. The photocatalytic degradation process enhances the uptake of dye molecules by the adsorbent. Therefore the adsorption capacity of the adsorbent (qmax*) will increase. Since the adsorption and photocatalytic degradation processes occur simultaneously, the adsorption affinity is a combination between chemical reaction process and chemical or physical adsorption. Therefore, energy of adsorption is a sum of isosteric heat of adsorption and heat of chemical reaction, now in the temperature dependent form the adsorption affinity can be written as KL ¼ KoLexp ?RQT þ ?ΔH RT (4) In Eq. (4), KL° is a Langmuir constant at reference temperature that combines both of adsorption and photocatalytic degradation process, R and T are ideal gas constant and temperature of adsorption, respectively. Isosteric heat of adsorption is represented by symbol Q and heat of chemical reaction is given by symbol ΔH . It is evident (Fig. 2) that not all the surface of bentonite in the composites are covered by TiO2 particles in where the photocatalytic degradation process occurs, and some part of the surface still available for only the adsorption process. If the available space for adsorption and photocatalytic degradation process is called as the active site; the fraction of the active site for adsorption alone is θad and for simultaneous adsorption and photocatalytic degradation is θdeg (Eq. (5)), θad þ θdeg ¼ 1 (5) Each of the available processes (adsorption or photocatalytic degradation) contributes a certain amount of energy on the adsorption affinity, the contribution is linear with the fraction of each active site, and Eq. (5) can be rewritten as Eq. (6): KL ¼ KoLexp ?RQT ?ΔH θad þ RT θdeg (6) ([]GIF\$DT)7_.giF 0.25 0.35 (a) (b) 0.30 0.20 0.25

```
7mmol/g 0. 15 0. 20 0.10 q e, mmol/g 0.
```

15 T = 30oC 0.10 0.05 T = 50oC T = 70oC 0.05 Modified Langmuir 0.00 0.00 0.0 0.1 0.2 0.3 0.4 0.5 0.0 0.1 0.2 0.3 0.4 0.5 Ce, mmol/L Ce, mmol/L 0.35 (c) 0.30 0.25 ge,

```
33mmol/g 0. 20 0. 15 0. 10 0. 05 0.00 0. 0 0. 1 0. 2 0. 3 0. 4 0. 5 Ce, mmol/L
```

Fig. 7. Adsorption isotherms and theoretical modified Langmuir model on the adsorption of MB under UV light irradiation. (a) B + 5% TiO2, (b) B + 10% TiO2, and (c) B + 20% TiO2. Substitution of Eq. (5) into (6) produces Eq. (7) KL ¼ KoLexp ?RQTθad þ ?RΔTHð1 ? θadÞ (7) The modified Langmuir equation for adsorption and photocatalytic degradation can be written as qe ¼ qmaxKoLexp ?RQTθad þ ?RΔTHð1 ? θad P Ce= 1 p KoLexp ?Q ?ΔH RT θad p RT δ1 ? θad Ce (8) Where qe* in Eq. (8) is the pseudo-total amount of dye adsorbed and degraded at equilibrium condition. Figs. 7 and 8 show the experimental adsorption data of MB and RhB onto composites under UV light irradiation. Theoretical plots of Eq. (8) are also given in those figures. It is evident that the modified Langmuir equation

31can represent the experimental adsorption data very well. The adsorption of MB and RhB onto

([]GIF\$DT)8_.giF 0.25 0.25 (a) (b) 0.20 0.20 qe,

```
5mmol/g 0.15 qe, mmol/g 0.15 0.10 0.10
```

T = 30oC T = 50oC 0.05 T = 70oC 0.05 Modified Langmuir 0.00 0.00 0.0 0.1 0.2 0.3 0.0 0.1 0.2 0.3 Ce, mmol/L Ce, mmol/L 0.25 (c) 0.20

```
11qe, mmol/g 0. 15 0. 10 0. 05 0. 00 0.0 0.1 0.2 0.3 Ce, mmol/L Fig. 8.
Adsorption
```

isotherms and theoretical modified Langmuir model on the adsorption of RhB under UV light irradiation. (a) B + 5% TiO2, (b) B + 10% TiO2, and (c) B + 20% TiO2. bentonite - TiO2 composites under UV light irradiation can enhance the "adsorption capacity" of the composites more than 30%. The parameters of modified Langmuir equation obtained from the fitting of the experimental data are summarized in Tables 3 and 4. It is evident that the ratio of TiO2 and temperature play a significant role in the removal of MB and RhB from aqueous solution. The adsorption and photocatalytic degradation of MB and RhB onto composites are endothermic processes as indicated by positive values of Q and ΔH (Tables 3 and 4). Since both of adsorption and photocatalytic degradation are endothermic processes, the increase of temperature enhanced the amount uptake and degradation reaction. In general, the values of Q and ΔH are essentially independent of temperature but dependent on the adsorption system as seen in Tables 3 and 4. This phenomenon is consistent with many adsorption systems [22, 23]. The photocatalytic degradation of MB and RhB is a function of TiO2 ratio. The fraction of the active site for photocatalytic degradation reaction (0deg) increased Table 3. Modified Langmuir

```
17parameters for the adsorption of MB
```

onto composites with UV irradiation. Adsorbent T (°C) Parameters

```
20qm* (mmol/g) KL° (L/mmol) Q (kJ/mol)
```

ΔH (kJ/mol) θad θdeg R2 B+ 5% TiO2 30 50 70 0.2034 0.2119 0.2228 863.07 1050.80 1229. 37 10.32 9.97 10.18 9.57 10.17 10.31 0.857 0.771 0.652 0.143 0.229 0.348 0.994 0.997 0.995 B+ 10% TiO2 30 50 70 0.2712 0.3253 0.3506 951.16 1215.62 1428.31 11.52 11.91 10.98 13.78 13.56 13.99 0.741 0.569 0.428 0.259 0.431 0.572 0.989 0.995 0.990 B+ 20% TiO2 30 50 70 0.3146 0.3423 0.3681 1098.75 1362.54 1567.85 12.34 12.02 11.98 14.96 15.02 14.75 0.539 0.401 0.298 0.461 0.599 0.702 0.986 0.989 0.991 Table 4. Modified Langmuir parameters for the adsorption of RhB onto composites under UV irradiation. Adsorbent T (°C) Parameters

20qm* (mmol/g) KL° (L/mmol) Q (kJ/mol)

ΔH (kJ/mol) θad θdeg R2 B+ 5% TiO2 30 50 70 0.1798 0.1938 0.2214 988.25 1205.25 1398.14 8.54 9.01 8.77 12.81 12.48 12.16 0.813 0.681 0.593 0.187 0.319 0.407 0.995 0.998 0.992 B+ 10% TiO2 30 50 70 0.2074 0.2296 0.2414 1078.45 1251.44 1458.05 10.32 9.88 10.20 14.02 13.75 14.21 0.711 0.531 0.493 0.289 0.469 0.507 0.987 0.991 0.989 B+ 20% TiO2 30 50 70 0.2189 0.2374 0.2594 1152.39 1369.59 1523.23 11.06 10.59 10.84 14.95 14.78 14.56 0.652 0.495 0.386 0.348 0.505 0.614 0.991 0.994 0.995 with the increase of TiO2 ratio. As mentioned before, the presence of TiO2 in the solid system will initiate the formation of ●OH radical and this radical acts as the active site for photocatalytic degradation reaction. With the increase in the number of TiO2 particles (an increase of TiO2 ratio), the number of free ●OH radical also increase, and it enhanced the photocatalytic degradation of MB and RhB. 4. Conclusion In this study, bentonite - TiO2 composites were prepared by impregnation followed by microwave irradiation processes. Physical characteristics

9of the composites were determined using FTIR analysis, XRD, SEM, and

nitrogen sorption methods. The adsorption and photocatalytic degradation capability of the composites were tested against MB and RhB solution. The liquid phase adsorption experiment was conducted with or without UV light irradiation. The UV light irradiation process can enhance the uptake or degradation of MB and RhB more than 30% of the process without UV light irradiation. Langmuir and Freundlich adsorption equations were employed to correlate the experimental adsorption data, and Langmuir model gave a better representation than Freundlich. To accommodate the photocatalytic degradation process into the adsorption isotherm, the modification of Langmuir equation by the inclusion of heat of reaction and fraction of the active site for photocatalytic degradation process was conducted. The modified Langmuir model can represent the experimental data well with reasonable parameters values. Declarations Author contribution statement Livy Laysandra and Meri Winda Masnona Kartika Sari: Performed the experiments. Felycia Edi Soetaredjo:

2Conceived and designed the experiments; Wrote the

paper. Kuncoro Foe, Jindrayani Nyoo Putro and Alfin Kurniawan:

2Analyzed and interpreted the data. Yi-Hsu Ju: Contributed reagents, materials, analysis tools or data; Wrote the paper.

Suryadi Ismadji: Conceived and designed the experiments; Contributed reagents, materials, analysis tools or data; Wrote the paper.

2Funding statement This work was supported by

the

16Indonesia Ministry of Research and Technology and Higher Education through Competency Grant

2Competing interest statement The authors declare no conflict of interest. Additional information No additional information is available for this paper.

References [1] W. Hajjaji, S.O. Ganiyu, D.M. Tobaldi, S. Andrejkovičová, F.R.R.C. Pullar, J.A. Labrincha, Natural Portuguese clayey materials and derived TiO2- containing composites used for decolouring methylene blue (MB) and orange II (OII) solutions, Appl. Clay Sci. 83-84 (2013) 91-98. [2] R. Djellabi, M.F. Ghorab, G. Cerrato, S. Morandi, S. Gatto, V. Oldani, A.D. Michele, C.L. Bianchi, Photoactive TiO2montmorillonite composite for degradation of organic dyes in water, J. Photochem. Photobiol. A: Chem. 295 (2014) 57-63. [3] H. Mittala, S.S. Raya, A study on the adsorption of methylene blue onto gum ghatti/TiO2 nanoparticles-based hydrogel nanocomposite, Int. J. Biol. Macromol. 88 (2016) 66-80. [4] S. Li, Removal of crystal violet from aqueous solution by sorption into semi- interpenetrated networks hydrogels constituted of poly(acrylic acid-acrylam- ide-methacrylate) and amylose, Biores. Technol. 101 (2010) 2197-2202. [5] A.A. Attia, B.S. Girgis, N.A. Fathy, Removal of methylene blue by carbons derived from peach stones by H3PO4 activation: Batch and column studies, Dyes Pigments 76 (2008) 282-289. [6] P. Sharma, H. Kaur, M. Sharma, V. Sahore, A review on applicability of naturally available adsorbents for the removal of hazardous dyes from aqueous waste, Environ. Monit. Assess. 183 (2011) 151-195. [7] V.K. Gupta, I. Ali, V.K. Saini, Removal of Rhodamine B, Fast Green, and Methylene Blue from Wastewater Using Red Mud, an Aluminum Industry Waste, Ind. Eng. Chem. Res. 43 (2004) 1740-1747. [8] W.S.W. Ngah, M.A.K.M. Hanafia, Removal of heavy metal ions from wastewater by chemically modified plant wastes as adsorbents: a review, Biores. Technol. 99 (2008) 3935–3948. [9] Y. Gao, Y. Wang, H. Zhang, Removal of Rhodamine B with Fe-supported bentonite as heterogeneous photo-Fenton catalyst under visible irradiation, Appl. Catal. B: Env. 78 (2015) 29-36. [10] V. Belessia, G. Romanosa, N. Boukosa, D. Lambropouloud, C. Trapalisa, Removal of Reactive Red 195 from aqueous solutions by adsorption on the surface of TiO2 nanoparticles, J. Hazard. Mater. 170 (2009) 836-844. [11] A. Kurniawan, H. Sutiono, N. Indraswati, S. Ismadji, Removal of basic dyes in binary system by adsorption using rarasaponin-bentonite: Revisited of extended Langmuir model, Chem. Eng. J. 189-190 (2012) 264–274. [12] N. Belhouchat, H. Zaghouane-Boudiaf, C. Viseras, Removal of anionic and cationic dyes from aqueous solution with activated organo-bentonite/sodium alginate encapsulated beads, Appl. Clay Sci. 135 (2017) 9-15. [13] J. Chanathaworn, C. Bunyakan, W. Wiyaratn, J. Chungsiriporn, Photocatalytic decolorization of basic dye by TiO2 nanoparticle in photoreactor, Songklanakarin J. Sci. Technol. 34 (2012) 203-210. [14] K. Nakataa, A. Fujishimaa, Design and applications, J. Photochem. Photobiol. A: Chem. 13 (2012) 169-189. [15] D.I. Petkowicz, R. Brambilla, C.U. Radtke, C.D.S. Silva, Z.N.d.R.B.C. Pergher, J.H.Z. Santos, Photodegradation of methylene blue by in situ generated titania supported on a NaA zeolite, Appl. Catal. A 357 (2009) 125-134. [16] B. Damardji, H. Khalaf, L. Duclaux, B. David, Preparation of TiO2-pillared montmorillonite as photocatalyst Part I. Microwave calcination, characterisa-tion, and adsorption of a textile azo dye, Appl. Clay Sci. 44 (2008) 201-205. [17] A.B. Dukic, K.R. Kumric, N.S. Vukelic, Z.S. Stojanovic, M.D. Stojmenovic, S.S. Milosevic, L.L. Matovic, Influence of ageing of milled clay and its composite with TiO2 on the heavy metal adsorption characteristics, Ceramic Int. 41 (2015) 5129-5137. [18] S. Ismadji, D.S. Tong, F.E. Soetaredjo, A. Ayucitra, W.H. Yu, C.H. Zhou, Bentonite hydrochar composite for removal of ammonium from Koi fish tank, Appl. Clay Sci. 119 (2016) 146-154. [19] K. Bahranowski, A. Gawel, A. Klimek, A. Michalik-Zym, B.D. Naprus- zewska, M. Nattich-Rak, M. Rogowska, E.M. Serwicka, Influence of purification method of Na-montmorillonite on textural properties of clay mineral composites with TiO2 nanoparticles, Appl. Clay Sci. 140 (2017) 75-80. [20] J. Henych, M. Kormunda, M. Stastny, P. Janos, P. Vomacka, J. Matousek, V. Stengl, Water-based synthesis of TiO2/CeO2 composites supported on plasma-treated montmorillonite for parathion methyl degradation, Appl. Clay Sci. 144 (2017) 26-35. [21] E. Rossetto, D.I. Petkowicz, J.H.Z.d. Santos, S.B.C. Pergher, F.G. Penha, Bentonites impregnated with TiO2 for photodegradation of methylene blue, Appl. Clay Sci. 48 (2010) 602-606. [22] F.P. Yesi, Y.H. Sisnandy, F.E. Ju, S. Soetaredjo, Ismadji, Adsorption of Acid Blue 129 from Aqueous Solutions onto Raw and Surfactant-modified Bentonite: Application of Temperature-dependent Forms of Adsorption Isotherms, Ads. Sci. Technol. 28 (2010) 847-868. [23] A. Kurniawan, A.N. Kosasih, J. Febrianto, Y.H. Ju, J. Sunarso, N. Indraswati, S. Ismadji, Utilization of rarasaponin natural surfactant for organo-bentonite preparation: Application for methylene blue removal from aqueous effluent, Chem. Eng. J. 172 (2011) 158-166. Article No~e00488 ([[GIF\$DT)2_giF Article No~e00488 ([[GIF\$DT)3_giF Article No~e00488 Article No~e00488 Article No~e00488 ([]GIF\$DT)5_.giF Article No~e00488 Ar Article No~e00488 Article No~e00488

142 http://dx.doi.org/10.1016/j.

heliyon.2017.e00488 2405-8440/©

22017 The Authors. Published by Elsevier Ltd.

This is an open access article

1under the CC BY-NC-ND license (http://creativecommons.org/licenses/bync-nd/4.0/). 3

3http://dx.doi.org/10.1016/j. heliyon .2017.

e00488 2405-8440/©

22017 The Authors. Published by Elsevier Ltd.

This is an open access article

1under the CC BY-NC-ND license (http://creativecommons.org/licenses/bync-nd/4.0/). 4

3http://dx.doi.org/10.1016/j. heliyon .2017.

e00488 2405-8440/©

22017 The Authors. Published by Elsevier Ltd.

This is an open access article

1under the CC BY-NC-ND license (http://creativecommons.org/licenses/bync-nd/4.0/). 5

3http://dx.doi.org/10.1016/j. heliyon .2017.

e00488 2405-8440/©

22017 The Authors. Published by Elsevier Ltd.

This is an open access article

1under the CC BY-NC-ND license (http://creativecommons.org/licenses/bync-nd/4.0/). 6

3http://dx.doi.org/10.1016/j. heliyon .2017.

e00488 2405-8440/©

22017 The Authors. Published by Elsevier Ltd.

This is an open access article

1under the CC BY-NC-ND license (http://creativecommons.org/licenses/bync-nd/4.0/). 7

3http://dx.doi.org/10.1016/j. heliyon .2017.

e00488 2405-8440/©

22017 The Authors. Published by Elsevier Ltd.

This is an open access article

1under the CC BY-NC-ND license (http://creativecommons.org/licenses/bync-nd/4.0/). 8 3http://dx.doi.org/10.1016/j. heliyon .2017. e00488 2405-8440/© 22017 The Authors. Published by Elsevier Ltd. This is an open access article 1under the CC BY-NC-ND license (http://creativecommons.org/licenses/by-3http://dx.doi.org/10.1016/j. heliyon .2017. e00488 2405-8440/© 22017 The Authors. Published by Elsevier Ltd. This is an open access article 1under the CC BY-NC-ND license (http://creativecommons.org/licenses/bync-nd/4.0/). 10 3http://dx.doi.org/10.1016/j. heliyon .2017. e00488 2405-8440/© 22017 The Authors. Published by Elsevier Ltd. This is an open access article 1under the CC BY-NC-ND license (http://creativecommons.org/licenses/bync-nd/4.0/). 11 3http://dx.doi.org/10.1016/j. heliyon .2017. e00488 2405-8440/© 22017 The Authors. Published by Elsevier Ltd. This is an open access article 1under the CC BY-NC-ND license (http://creativecommons.org/licenses/bync-nd/4.0/). 12

```
3http://dx.doi.org/10.1016/j. heliyon .2017.
```

e00488 2405-8440/©

```
22017 The Authors. Published by Elsevier Ltd.
```

This is an open access article

1under the CC BY-NC-ND license (http://creativecommons.org/licenses/bync-nd/4.0/). 13

3http://dx.doi.org/10.1016/j. heliyon .2017.

e00488 2405-8440/©

22017 The Authors. Published by Elsevier Ltd.

This is an open access article

1under the CC BY-NC-ND license (http://creativecommons.org/licenses/bync-nd/4.0/). 14

3http://dx.doi.org/10.1016/j. heliyon .2017.

e00488 2405-8440/©

22017 The Authors. Published by Elsevier Ltd.

This is an open access article

1under the CC BY-NC-ND license (http://creativecommons.org/licenses/bync-nd/4.0/). 15

3http://dx.doi.org/10.1016/j. heliyon .2017.

e00488 2405-8440/©

22017 The Authors. Published by Elsevier Ltd.

This is an open access article

1under the CC BY-NC-ND license (http://creativecommons.org/licenses/by-

1416 http://dx.doi.org/10.1016/j.

heliyon.2017.e00488 2405-8440/©

22017 The Authors. Published by Elsevier Ltd.

This is an open access article

1under the CC BY-NC-ND license (http://creativecommons.org/licenses/bync-nd/4.0/).

1417 http://dx.doi.org/10.1016/j.

heliyon.2017.e00488 2405-8440/©

22017 The Authors. Published by Elsevier Ltd.

This is an open access article

1under the CC BY-NC-ND license (http://creativecommons.org/licenses/bync-nd/4.0/).

1418 http://dx.doi.org/10.1016/j.

heliyon.2017.e00488 2405-8440/©

22017 The Authors. Published by Elsevier Ltd.

This is an open access article

1under the CC BY-NC-ND license (http://creativecommons.org/licenses/bync-nd/4.0/).

19 http://dx.doi.org/10.1016/j.heliyon.2017.e00488 2405-8440/© 2017 The Authors. Published by Elsevier Ltd. This is an open access article under the CC BY-NC-ND license (http://creativecommons.org/licenses/bync-nd/4.0/). 20 http://dx.doi.org/10.1016/j.heliyon.2017.e00488 2405-8440/© 2017 The Authors. Published by Elsevier Ltd. This is an open access article under the CC BY-NC-ND license (http://creativecommons.org/licenses/by-nc-nd/4.0/). 21 http://dx.doi.org/10.1016/j.heliyon.2017.e00488 2405-8440/© 2017 The Authors. Published by Elsevier Ltd. This is an open access article under the CC BY-NC-ND license (http://creativecommons.org/licenses/by-nc-nd/4.0/). 22

http://dx.doi.org/10.1016/j.heliyon.2017.e00488 2405-8440/© 2017 The Authors. Published by Elsevier Ltd. This is an open access article under the CC BY-NC-ND license (http://creativecommons.org/licenses/by-ncnd/4.0/).